PD CF 0305

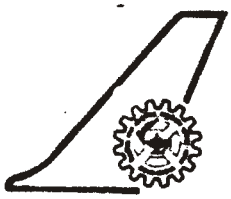

National
Aerospace
Laboratories

Natural Convection in a Cubical Cavity: Case of Multiple Solutions

M D DESHPANDE
Computational & Theoretical Fluid Dynamics Division

Project Document CF 0305

July 2003
Bangalore 560 017, India

Natural Convection in a Cubical Cavity: Case of Multiple Solutions

1. Introduction

The purpose of this report is to study an interesting case of natural convection in a cubical cavity. A set of boundary conditions has been applied on the six walls and the buoyancy driven flow inside the cavity is due to the heating of the bottom wall. Interestingly two families of distinct steady solutions have been observed. Both the families have the same critical Rayleigh number $(Ra)_{crit}$ below which there is no flow and heat transfer is by pure conduction.

The Navier-Stokes and the energy equations under the Boussinesq approximation are solved numerically by a time marching technique. Two distinct solutions for a set of identical boundary conditions came as a surprise to us. In an earlier report (Deshpande 2003) several combinations of boundary conditions had been studied. The classical Rayleigh-Benard convection problem was also modelled in that study for a single square cell. This problem has been studied extensively (see, for example, Chandrasekhar (1961), Reid & Harris (1958, 1959), Palm (1960), Segel & Stuart (1962) and Stuart (1964)).

It may be specially noted here that the linear stability theory is usually employed to study the Rayleigh-Benard problem and it cannot predict the cell shape. Even though three shapes - equilateral triangle, square and regular hexagon - have been considered as possible candidates, hexagonal shape seems to be the preferred candidate. But no mention of multiple solutions is suspected in any of the studies mentioned above. Multiple solutions, however, have been reported by Kuhlmann et al (1997) for the case of lid-driven cavity where there is no heating but driving is two-sided. Multiple solutions we are going to report here may be of great engineering importance where convective heat transfer is involved. See, for example, Jaluria(2001).

In the earlier report by Deshpande (2003) mentioned above extensive testing of the numerical methods and other computational details are documented. We refer to that report and give only the essential details here for the sake of completeness. The focus here is going to be on the main results that show the multiplicity of the results under steady state conditions.

2. Formulation of the problem

The geometry of the rectangular parallelepiped and the coordinate axes are shown in figure 1. The dimension of the container are l'_x, l'_y, and l'_z with l'_x being measured in the vertical direction. It is filled with an incompressible, newtonian fluid of density ρ and kinematic viscosity ν.

The geometry chosen in this study is a cubical cavity with $l'_x = l'_y = l'_z$. Each of the six walls being a solid wall, no-slip velocity boundary condition is applied on them. The bottom wall at $x' = l'_x$ is kept at temperature T'_2 and the top wall is kept at $T'_1 < T'_2$. Other four vertical side walls are insulated and thus satisfy the condition that the normal temperature derivative is zero. A problem that is closely related to this case was reported in Deshpande (2003) (case C). The geometry in that case was

also cubical and heating was done from below. Only difference in that case was that the side walls were maintained at the constant temperature of the top wall T_1' which amounts to non-dimensional value of zero. We will see that the present change in the side wall temperature boundary condition will lead to interesting differences.

We will write down the governing equations in their non-dimensional form. Dimensional variables are indicated by a prime. Thus (x', y', z') are the dimensional variables, with x' being measured downwards as shown in figure 1. The depth of the container l_x', reference velocity $v_{ref} = \nu/l_x'$ are the length and velocity scales used to non-dimensionalize. Quantities without primes are the non-dimensional variables. Hence

$$(x, y, z) = (x', y', z')/l_x'$$

$$(u, v, w) = (u', v', w')/v_{ref} = (u', v', w')l_x'/\nu$$

$$\tau = t\nu/l_x'^2$$

$p = \frac{p'}{\rho v_{ref}^2}$ pressure deviation from hydrostatic pressure

$\theta = \frac{T'-T_1'}{T_2'-T_1'} = \frac{T'-T_1'}{\Delta T'}$ Temperature,

where $\Delta T' = T_2' - T_1'$ with T_1' & T_2' being two boundary values.

Other related variables are -

β = Coefficient of expansion = $\frac{1}{T'}$, for a perfect gas.
$\beta(T' - T_0')$= Relative change of volume
k = Thermal conductivity
$\alpha = k/(\rho C_p)$ Thermal diffusivity
$Pr = \mu.C_P/k$ Prandtl number
$Ra = g\beta \mid T_2' - T_1' \mid l_x'^3/(\nu\alpha)$ Rayleigh number, with gravity g acting downward along the x-direction.
$Gr = Ra/Pr$ Grashof number.

With these variables the governing equations of continuity, momentum and energy are written with $\overrightarrow{u}$=(u, v, w)

$$D = \nabla.\overrightarrow{u} = 0 \tag{2.1}$$

$$\frac{\partial \overrightarrow{u}}{\partial \tau} + (\overrightarrow{u}.\nabla)\overrightarrow{u} = -\nabla p + \nabla^2\overrightarrow{u} - \hat{e}_x\frac{Ra}{Pr}\theta \tag{2.2}$$

$$\frac{\partial \theta}{\partial \tau} + (\overrightarrow{u}.\nabla)\theta = \frac{1}{Pr}\nabla^2\theta. \tag{2.3}$$

We will solve a Poisson equation for pressure which is derived by taking the divergence of equation (2.2)

$$\nabla^2 p = -\frac{\partial D}{\partial \tau} - \nabla.[(\overrightarrow{u}.\nabla)\overrightarrow{u}] + \nabla^2 D - \frac{Ra}{Pr}\frac{\partial \theta}{\partial x}. \tag{2.4}$$

In equation (2.4), $D = 0$ but it is retained for stability reasons (see Harlow & Welch (1965)).

3. Numerical Solution

The finite difference numerical solution procedure employed to solve equations (2.2) - (2.4) is sketched only briefly here since the details are reported in Deshpande (2003). We use the well known Marker and Cell (MAC) method and the staggered grid as proposed by Harlow & Welch (1965). An important improvement adopted here is the third order upwind scheme suggested by Kawamura & Kuwahara (1985). This scheme has good stability characteristics and maintains at the same time third order accuracy of the convective terms.

In the staggered grid arrangement, the pressure and temperature are stored at the cell centre and at the centre of each face of the cell is specified the velocity component normal to the face (see figure 1b). The grid is extended beyond each wall to take care of the boundary conditions. Equations 2.2 & 2.3 are solved by time marching using the Euler explicit method and equation 2.4 is solved iteratively for p.

Central difference scheme is used to approximate all the terms except the convective terms which are approximated by the third order upwind scheme as mentioned above. To maintain this high order of accuracy the boundary conditions are also approximated by second order schemes. Thus the overall accuracy of the numerical scheme is second order in space and first order in time.

4. Results and Discussion

The computational procedure discussed here has been tested extensively and some of the test results have been reported in Deshpande (2003). Grid independence study and tests to check the adequacy of other computational parameters like time increment $\triangle\tau$ have been conducted successfully. A (44 x 44 x 44) uniform cartesian grid was found to be satisfactory. Five cases were studied and two of them pertained to the classical Rayleigh-Benard problem (see Chandrasekhar 1961): A layer heated from below and both the bounding surfaces being rigid in the first case and being free in the second. Critical value of the Rayleigh number to start the motion is known from the linear stability theory. Ability to predict this value accurately is a good testimony to the reliability of the present numerical procedure.

The problem considered in this study has been described in section 2. In terms of the non-dimensional variables it amounts to a cube of unit dimension and the bottom wall heated to $\theta = 1$ and the top wall maintained at $\theta = 0$. The four vertical side walls are insulated. No-slip boundary condition is applied at all the six walls. The value of Pr is kept at 1.

We will show a set of results in figures 2 & 3 pertaining to a family of solutions and at $Ra = 7,000$. Flow is supercritical for this value of Ra and hence fluid is set into motion and the results shown in these figures are for the steady state. Quite interestingly another steady state solution has been observed for the same boundary conditions. Results pertaining to the second set are shown in figures 4 & 5. The two sets of solutions will be compared subsequently and we will see that we have a family of two solutions as Ra is changed. These will be identified as family A and family B, respectively.

4.1 Family A solution

In figure 2a is shown the streamline pattern in the vertical diagonal plane ($y = z$). This plane is specifically selected because the streamlines in this plane remain there forever as shown by a typical streamline. This plane divides the cube into two symmetrical prismatic cylinders each with a right-angled triangle base. The spiralling out streamline indicates that the fluid motion is towards the focus from both the sides and spiralling in the same sense (clockwise or counter clockwise). Hence we have a horizontal filament on either side of the plane, which is surrounded by spiralling fluid and is perpendicular to this symmetry plane. This picture can be understood better from figure 2b where two streamlines are shown, one on either side of the vertical symmetry plane. Flow is towards the centre of the cube from around the middle of two vertical edges ($y = 0, z = 1$) and ($y = 1, z = 0$). This spiraling flow spreads out near the symmetry plane ($y = z$) and then moves back along the walls.

Temperature contours corresponding to this flow are shown in figures 3a & 3b in the vertical planes $z = 0.25$ and $z = 0.5$, respectively. If Ra were subcritical the temperature contours would be horizontal surfaces $x =$ constant and they would show up as horizontal lines in the $z-$planes such as in these figures. But in figures 3a & 3b the contours have been pushed in the direction of the velocity, upwards near $y = 0$ and downwards near $y = 1$. Temperature contours in y-planes are similar to those in the corresponding z-planes and hence are not shown.

Before we move to the next section to present another solution that has been identified to belong to family B, it should be noted that these two families of solutions are distinctly different. In the present family A itself trivially different solutions are available because of symmetry which we do not distinguish from each other. For example, the vertical plane $y = z$ can be replaced by $y + z = 1$ as the symmetry plane. Sense of rotation of the pair of two vortices can be inter-changed between clockwise and counter clockwise. But in these four cases grouped into family A, the vortices on either side of the plane of symmetry would be spinning in the same direction and the streamlines spiraling out in the plane of symmetry. Hence there is not any intrinsic difference among these solutions and we group them as one solution. They can be obtained from each other by proper reflection or rotation. We have made no attempts to see if all the four of them are supported by the present numerical scheme even though in principle they should be. Subtle differences in the numerical scheme, for example the initial conditions or the direction in which we sweep the iteration of the pressure equation, may lead to a preference for a particular solution from this set. Even though we group these four solutions in family A together we go back to them later in the bifurcation diagrams since they may be of practical importance.

We will see that the solutions in family B are distinctly different from the present set.

4.2 Family B solution

In figure 4 are shown the streamlines for the same set of boundary conditions as in the previous case and also for the same values $Ra = 7000, Pr = 1$. But we see a different solution here and this belongs to what has been named as family B. Now the vertical plane $y = 0.5$ is a plane of symmetry and the flow consists of two toroidal vortices, one on each side of this plane. A streamline on this plane of symmetry remains on it only. The flow direction around the vortex centre is towards the plane of symmetry on both the sides and both the vortices spin in the same sense (either clockwise or counter clockwise). Temperature contours in two planes $z = 0.25$ and $z = 0.5$ are shown in figures 5a and 5b. We see a distortion of the temperature field from linearity due to the velocity field, contours being pushed in the direction of velocity. The contours are symmetrical in y about $y = 0.5$ plane. In frame (a) corresponding to $z = 0.25$ plane velocity is generally upwards along the negative x-direction and hence the temperature contours are pushed in that direction. In $z = 0.75$ plane, not shown here, they are pushed downwards. In $z = 0.5$ plane in frame (b) they are symmetrical in x.

We may repeat that there are other symmetrical solutions possible for this case also and we are not considering them separately. For example, instead of $y = 0.5$ being the plane of symmetry $z = 0.5$ can be the plane of symmetry. Also the sense of rotation of the two vortices can be interchanged, but both of them should rotate in the same direction. At the plane of symmetry the streamlines should spiral out indicating that the flow direction around the vortex centre is towards this plane on both the sides. Even though the symmetrical solutions in this family are grouped together, the differences may be of practical importance. We will address this question in the bifurcation diagrams in figure 10.

A quantitative comparison of the two distinct solutions is made by plotting u component of velocity on the line $x = z = 0.5$ in figure 6a, v component of velocity along the line $y = z = 0.5$ in figure 6b, w component of velocity along the line $x = y = 0.5$ in figure 6c and temperature along the line $y = z = 0.5$ in figure 6d. Because of symmetry mentioned earlier u and v components are zero for family B and other functions are odd functions in the respective variables as shown. Both u and v being zero for solution B in figures 6a & 6b indicates that vortex centreline coincided with the geometrical centre of $x - z$ plane as was seen figure 4. However, non zero value of w component of velocity in figure 6(c) indicates that the vortex is not rotationally symmetrical. For solution A the vortex centre is along a diagonal line (see figure 2) and hence u and v are non-zero in figures 6a & 6b. Specially notworthy is the temperature profiles in figure 6d which look so close to each other on this line even though contour shapes are much different as seen from figures 3b and 5b.

In figure 7 are shown the velocity and temperature profiles along the three centre-lines of the cube for family A solution for $Ra = 7500$ and $Pr = 1$. Similar plots for family B but for a slightly lower value of $Ra = 6000$ are shown in figure 8. These two sets of figures along with the previous streamlines and the contour plots should help in getting a good feel for the flow and temperature field.

4.3 The Critical Rayleigh Number

For the set of boundary conditions chosen for the cubical box in this problem there is a critical value of Rayleigh number $(Ra)_{crit}$ below which there is no fluid motion and heat transfer is by conduction alone. This is because of fluid viscosity and absence of gradients in the boundary conditions in the horizontal direction. Hence the flow can be stable for sufficiently low values of Rayleigh number.

Results shown in the previous figures for the two families were for the supercritical values of $Ra = 6,000 - 7,500$. Steady velocity and temperature fields were attained for both the cases. In the earlier study in Deshpande(2003) determination of the critical Rayleigh number for two cases of the Rayleigh-Benard problem was successfully achieved. Based on that experience computations were done for both the families of solutions. Convergence becomes slow near the critical value of Ra and computations should be continued sufficiently long to assure whether a chosen Ra is subcritical or supercritical. In a very slowly changing temperature field observation of the velocity at a few locations may mislead whether it is growing or not. Hence it is quite important to make sure that the temperature field also has reached the steady state.

Wall temperature at $z = 0$, $x = y = 0.5$ is shown as a function of Ra in figure 9. This value is distinctly different for the two families of solutions. We may recall that for family A a vertical diagonal plane is the plane of symmetry dividing the cube into two halves and for family B, on the other hand, a central plane perpendicular to either y or z axis like $y = 0.5$ or $z = 0.5$ is the symmetry plane. From the previous plots we know that for $Ra < (Ra)_{crit}$ heat transfer is by conduction only and this wall temperature has to be 0.5. For $Ra > (Ra)_{crit}$ convection sets in and the temperature at the monitoring point increases rapidly at first and asymptotically later. For the values of Ra upto 7,500 studied here flow reached a steady condition. In the neighbourhood of $(Ra)_{crit}$ an increment of 0.1 in Ra was used.

It was observed that for $Ra = 3386.7$ and lower values velocities decreased to very low values and remained there so that it can be considered as numerical noise. For $Ra = 3386.8$ and higher values velocity grew to reach a final steady state value. Hence we conclude $(Ra)_{crit} = 3386.75 \pm 0.25$. Uncertainty value of ± 0.25 is taken here from Deshpande (2003) for the Rayleigh-Benard cell case where both the boundary surfaces were considered to be rigid. The critical Ra value predicted there was 1707.5 which underpredicts the value of 1707.762 obtained from the linear stability theory.

Birfucation diagram shown for $\theta(x = 0.5, y = 0.5, z = 0)$ in figure 9 was for two distinct families of solutions A and B and ignored symmetrical solutions that can be obtained by reflection or rotation. But in reality these solutions are relevant too since if we put a probe, which is a thermometer in this case, any one of these solution may be obtained. Then the modified bifurcation diagram is shown in figure 10a. Wall temperature now can be any one of the two values from family A and any one of the three solutions from family B. It is interesting to note that for $Ra < (Ra)_{crit}$ the value of $\theta = 0.5$ is for pure conduction but for $Ra > (Ra)_{crit}$ the same value is also attained for the convection case in family B. Actually this figure is a degenerate case since the four solutions in family A have merged into two and two solutions of the four in family B have merged into one leading to $\theta = 0.5$. The most general case is shown schematically in figure 10b. Here each family has four possible solutions and a probe, say a thermometer or a velocity probe like laser Doppler anemometer in the field, will measure any one of the eight values. Out of these eight possible solutions, we

have seen before that only two are intrinsically distinct and are called here as multiple solutions of the N-S equations and the other three in each set are merely manifestations of symmetry. Nevertheless they are of engineering importance and hence are shown in figure 10b.

In figure 11 are shown some streamline patterns for $Ra = 3388$. This value of Ra is only slightly above the critical value and the temperature field is almost the same as that obtained from conduction. Hence it is very close to what one gets by linear interpolation between planes $x = 0$, $(\theta = 0)$ and $x = 1$, $(\theta = 1)$. Hence $\theta =$ x are the constant temperature surfaces for both family A and family B solutions. These show up as horizontal lines in z and y planes and may be compared with the distorted contour lines in figures 3 & 5. But the velocity field is already set in and qualitatively it is similar to what we have seen earlier for $Ra = 7000$. Since the flow is very close to the equilibrium case, velocities involved are very small and when a streamline takes a loop, even a complicated 3-dimensional one, it is displaced only by a small amount. That is why we see tightly wound loops of the streamlines in frames 11(a), (b) and (c) for the solution of family A and in frame 11(d) for the solution of family B. As before in the plane of symmetry $y = z$ in the first three frames the streamlines spiral out thus indicating a flow towards this plane at the vortex centre. Thus in frame (c), the streamline should gradually drift towards the edge $y = 0$, $z = 1$. In frame (d) the streamline points towards the mid symmetry plane $y = 0.5$.

5. Conclusion

Free convection in a cubical cavity heated from below has been studied in this report. Time accurate numerical solutions of the Navier-Stokes equations have been obtained under the Boussinesq approximation. No-slip condition is applied at the six walls and the four vertical side walls are insulated. Temperature difference with $\theta = 1$, 0 at the bottom and top walls drives the flow if Ra is greater than the critical value which has been determined numerically to be $(Ra)_{crit} = 3386.75 \pm 0.25$.

More interestingly, for the supercritical values of Ra two distinct solutions have been obtained. In what has been called solution A, the cube is divided into two symmetrical halves by a vertical diagonal plane and the streamlines in this plane spiral out. The flow in either half is such that it is towards the focus of this spiral. Corresponding to the same boundary conditions another solution has been found where a symmetry plane, this time a vertical central plane of the cube, divides the cube into two halves. This is solution B which consists of two toroidal vortices located symmetrically on either side and the flow at their centre being towards the plane of symmetry. The solutions A and B are distinctly different and each set, because of symmetry, consists of four solutions which can be obtained by rotation or reflection appropriately and they are not considered separately here but are grouped into a single solution or a family of solution.

In the analysis of the classical Rayleigh-Benard problem by the linear stability theory the cell shape and flow direction remain indeterminate even though the hexagonal shape remains to be the preferred shape. But no multiplicity of solutions has been suspected there. In the present case we have the distinct cubical shape with no-slip conditions on the walls and still get two distinct families of solutions.

Recognition of the multiple solutions and the ability to compute them may be important in many fields of engineering where convective heat transfer is involved like

crystal formation from melts, manufacture of semiconductors and metal casting.

I would like to thank Dr. S. Majumdar for helpful comments and Mr. B.G. Srinidhi, Mrs. D. Shobha, Mrs. L. Vijayalakshmi and Mr. Mallikarjun for their help in the preparation of the manuscript.

References

1. Chandrasekhar, S. (1961) Hydrodynamic and Hydromagnetic stability. Oxford at the Clarendon Press.

2. Deshpande, M.D.(2003) Free convection in a three-dimensional cavity. NAL Project Document PD CF 0303.

3. Harlow, F.H. & Welch, J.E. (1965) Numerical calculation of time-dependent viscous incompressible flow of fluid with free surface. Physics of Fluids, **8**, 2182-2189.

4. Jaluria, Y.(2001) Fluid Flow phenomena in material processing - The 2000 Freeman Scholar Lecture. J. of Fluids Engg. **123**, 173-210.

5. Kawamura, T. & Kuwahara, K. (1986) Computation of high Reynolds number flow around a circular cylinder with surface roughness, Fluid Dynamics Research, **1**, 145-162

6. Kuhlmann, H.C, Wanschura, M. & Rath, H.J(1997) Flow in two-sided lid-driven cavities: non-uniqueness, instabilities, and cellular structures. J. Fluid Mech. **336**, 267-299.

7. Palm, E. (1960) On the tendency towards hexagonal cells in steady convection. J.Fluid

   Mech. **8**, 183-192.

8. Reid, W. H. & Harris, D. L. (1959) Streamlines in Benard convection cells. Physics of Fluids, **2**, 716-717.

9. Reid, W.H. & Harris, D.L. (1958) Some further problems on the Bernard problem. Physics of Fluids, **1**, 102-110.

10. Segel, L.A. & Stuart, J.T. (1962) On the question of the preferred mode in cellular thermal convection. J.Fluid Mech. **13**, 298-306.

11. Stuart, J.T. (1964) On the cellur patterns in thermal convection. J.Fluid Mech.**18**, 481-498.

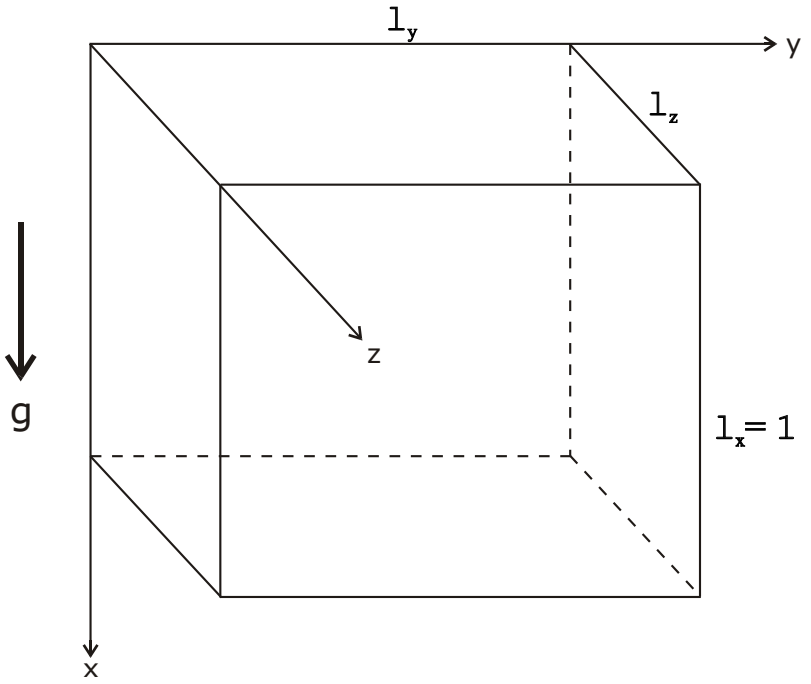

Figure 1(a) Geometry of the cavity.

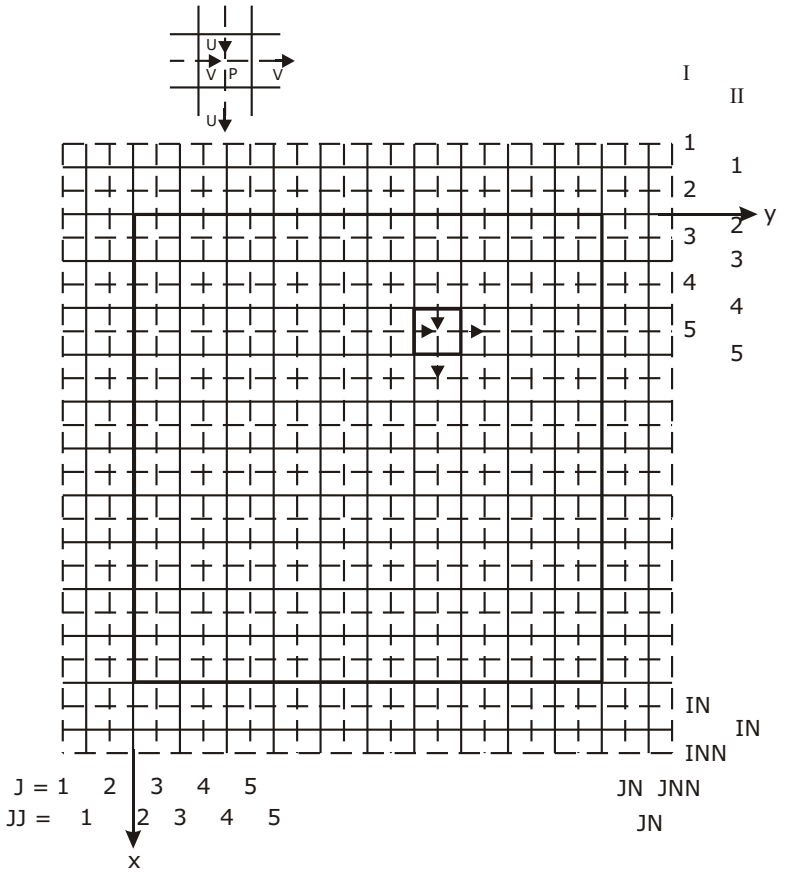

Figure 1(b) The staggered grid and specification of velocity components and pressure. The z-direction is not shown for simplicity.

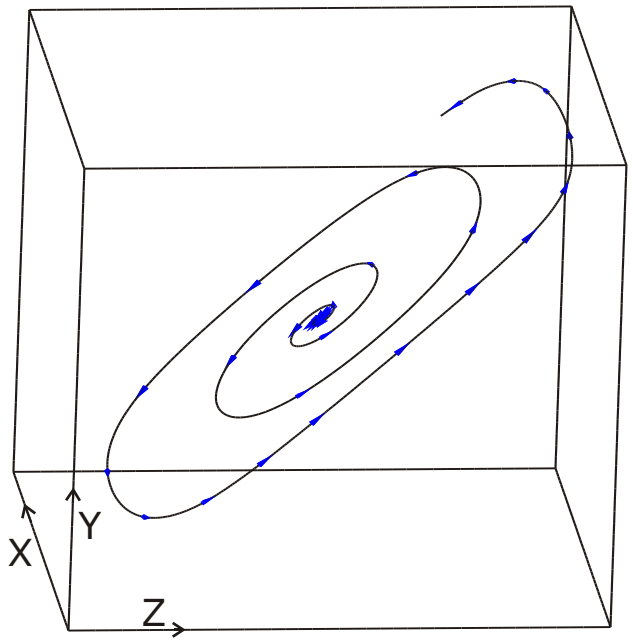

Figure 2. Streamlines for solution A. *Ra*=7000, *Pr*=1.0.
(a) Streamline in the vertical symmetry plane *y*=*z*.

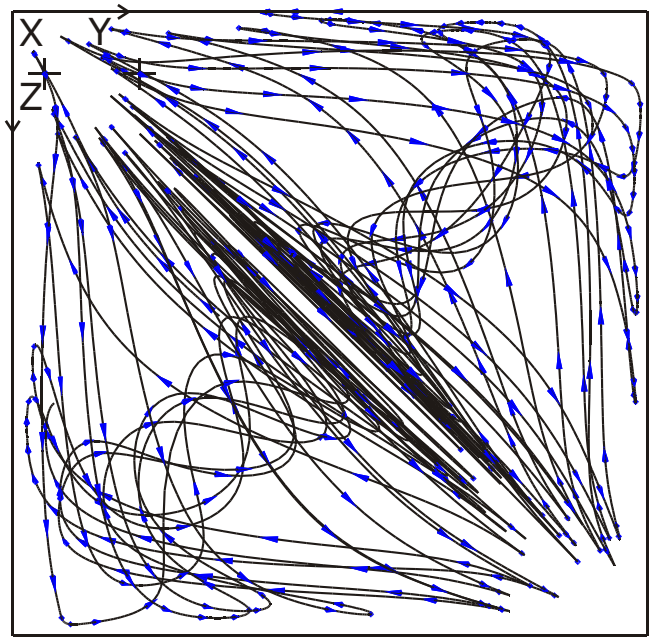

Figure 2(b) Two Streamlines indicating two vortices.

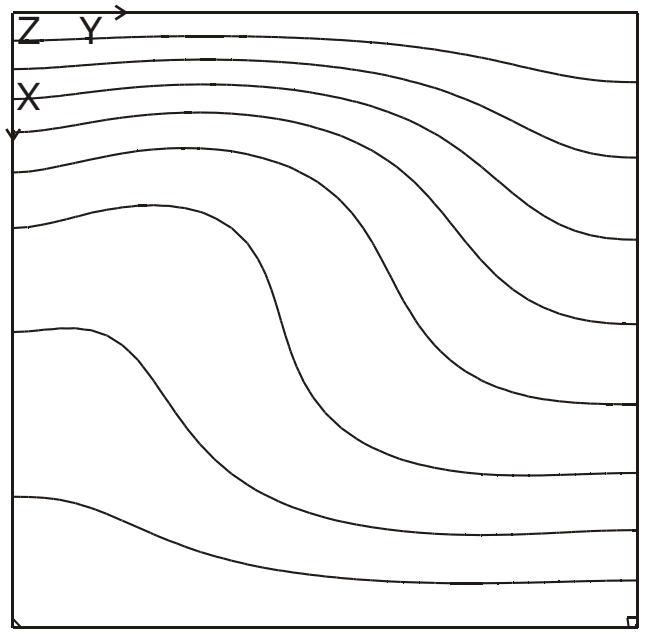

Figure 3. Temperature contours for solution A.
Ra=7000, *Pr*=1. (a) On plane *z*=0.25.

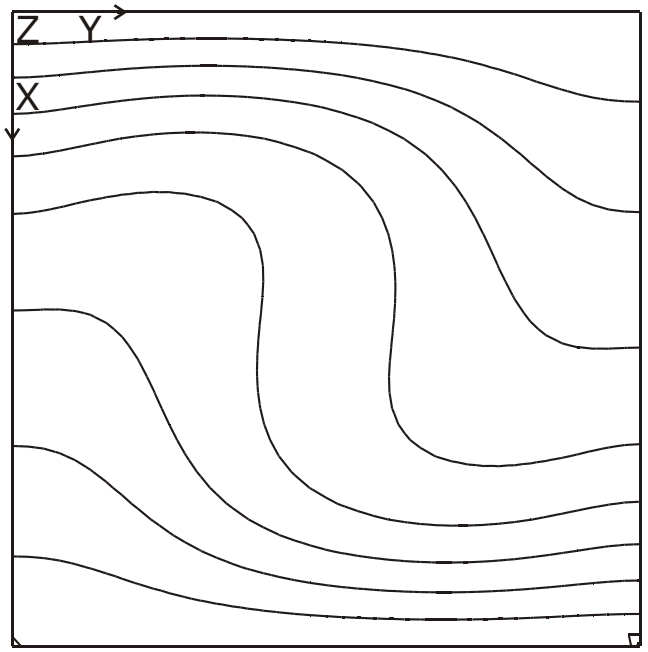

Figure 3(b) On plane *z*=0.5.

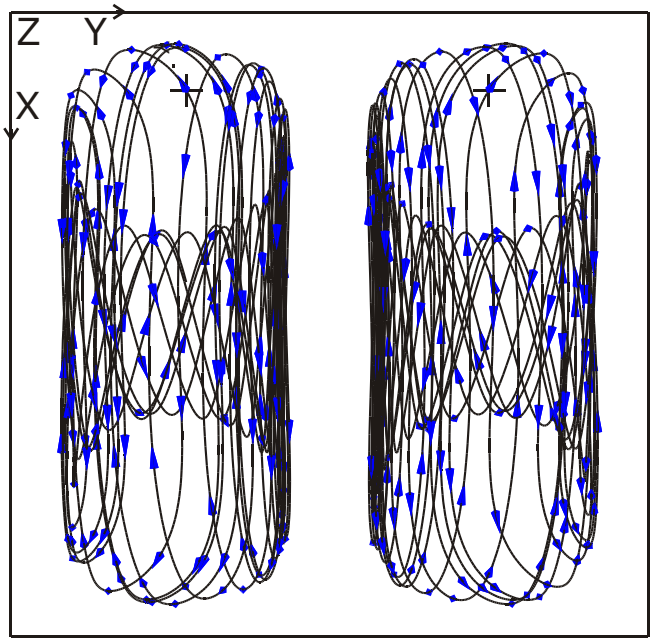

Figure 4. Streamlines for solution B. *Ra*=7000, *Pr*=1. (a) Two vortices on either side of the symmetry plane *y*=0.5.

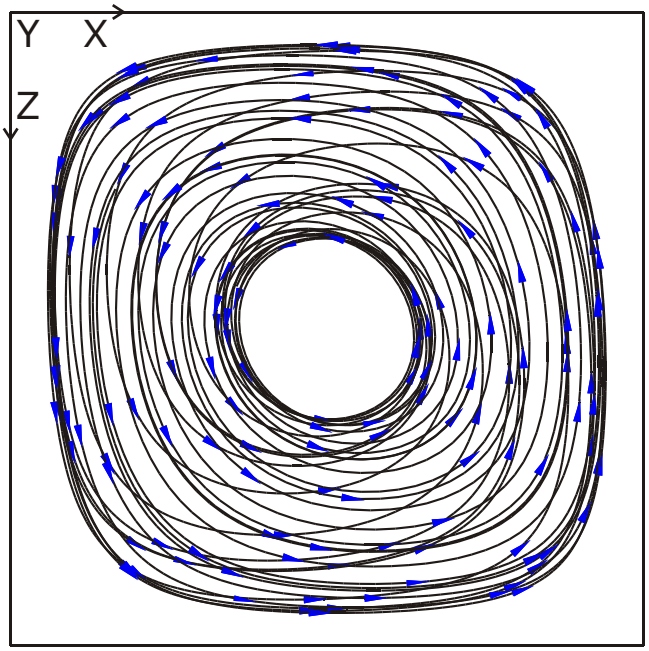

Figure 4(b) The same vortices located one behind the other.

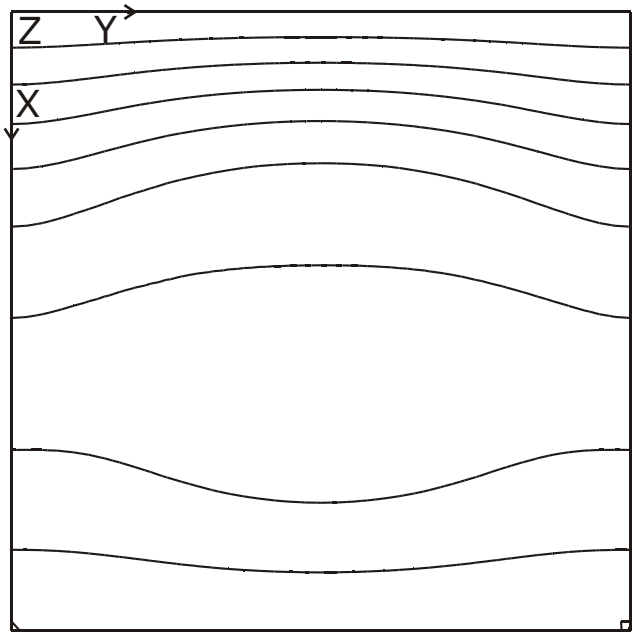

Figure 5. Temperature contours for solution B. *Ra*=7000, *Pr*=1.0. (a) On plane *z*=0.25.

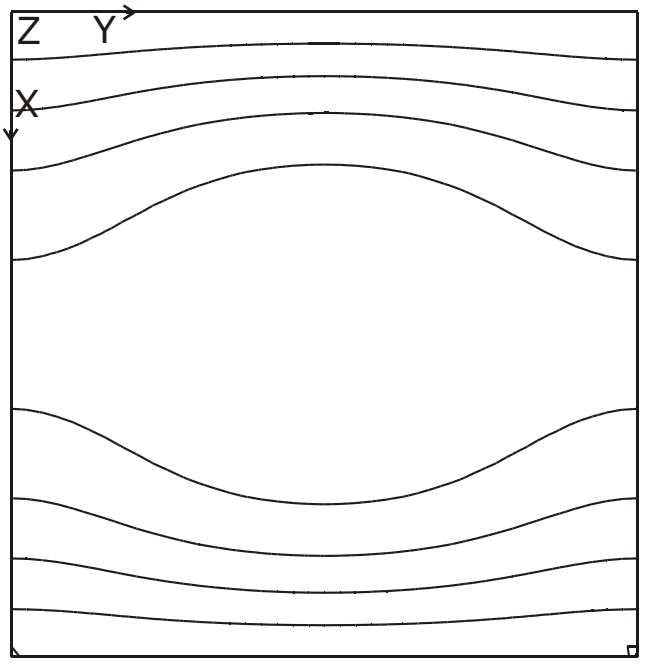

Figure 5(b) On plane *z*=0.5.

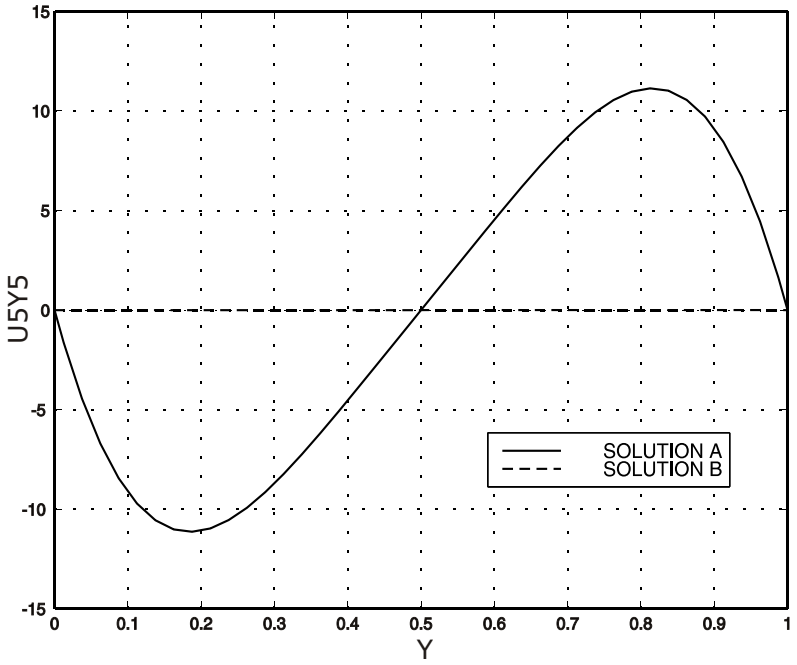

Figure 6. Comparison of profiles between solutions A & B. *Ra*=7000, *Pr*=1.0. (a) *u* velocity on the centreline *x*=0.5, *z*=0.5.

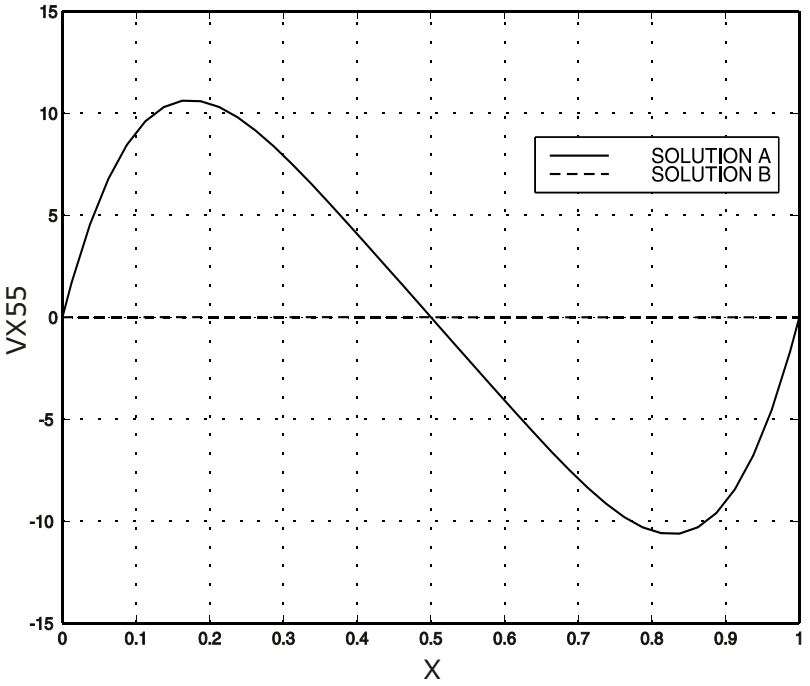

Figure 6(b) *v* velocity on the centreline y=*z*=0.5.

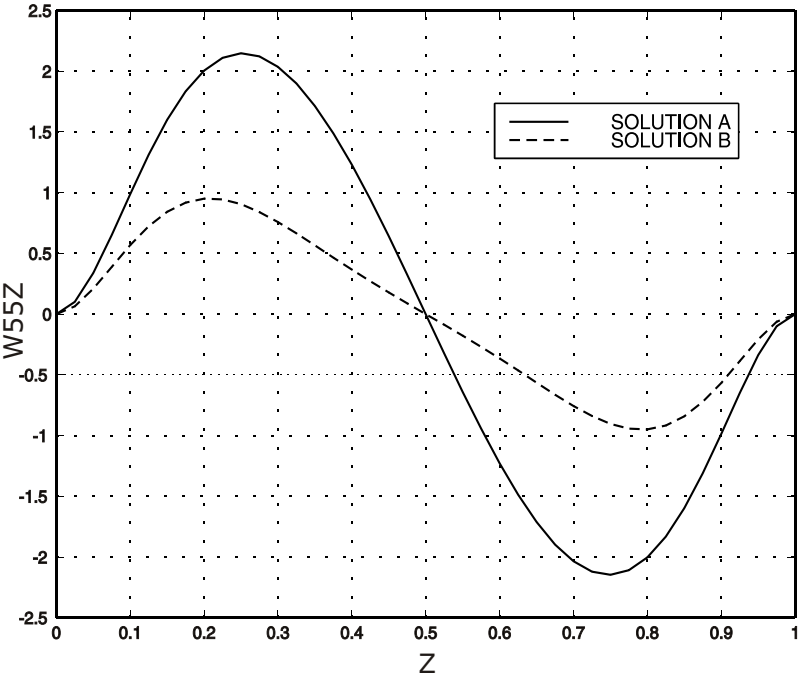

Figure 6(c) *w* velocity on the centreline $x=y=0.5$.

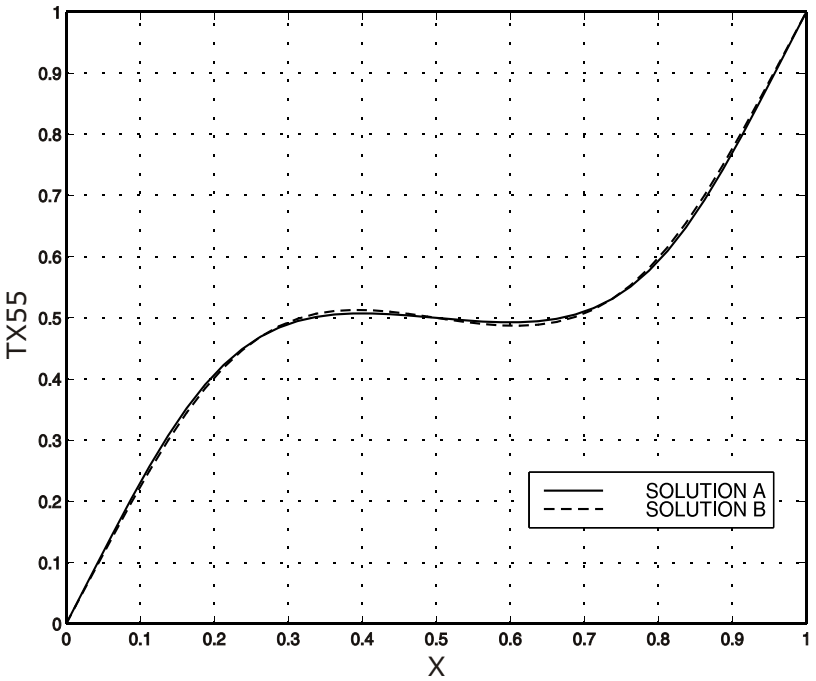

Figure 6(d) Temperature on the centreline $y=z=0.5$.

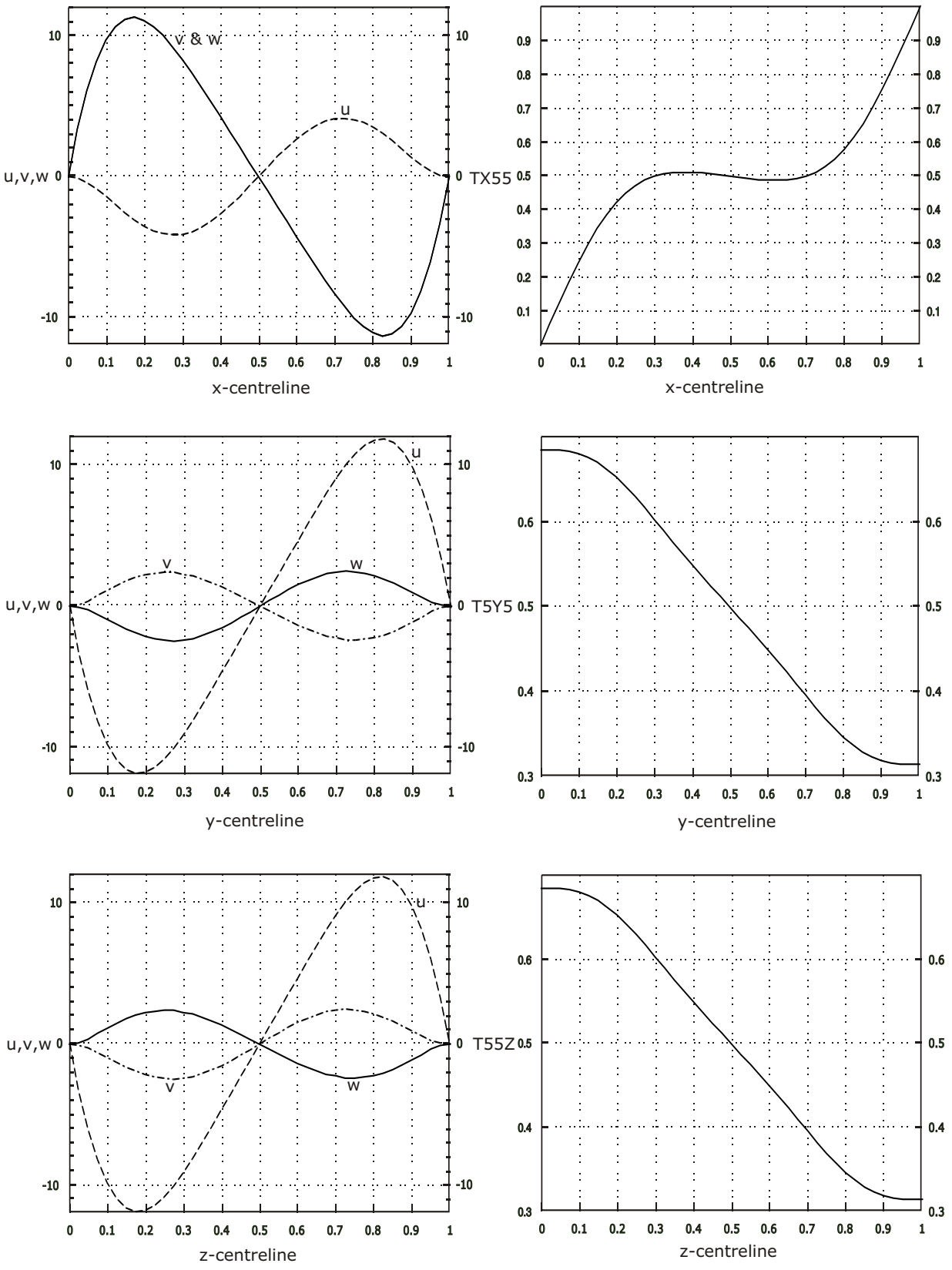

Figure 7. Velocity and temperature profiles on the centrelines of the cube for solution corresponding to family A. *Ra*=7500, *Pr*=1.0. Frames to the left indicate velocity profiles and frames to the right indicate temperature profiles.

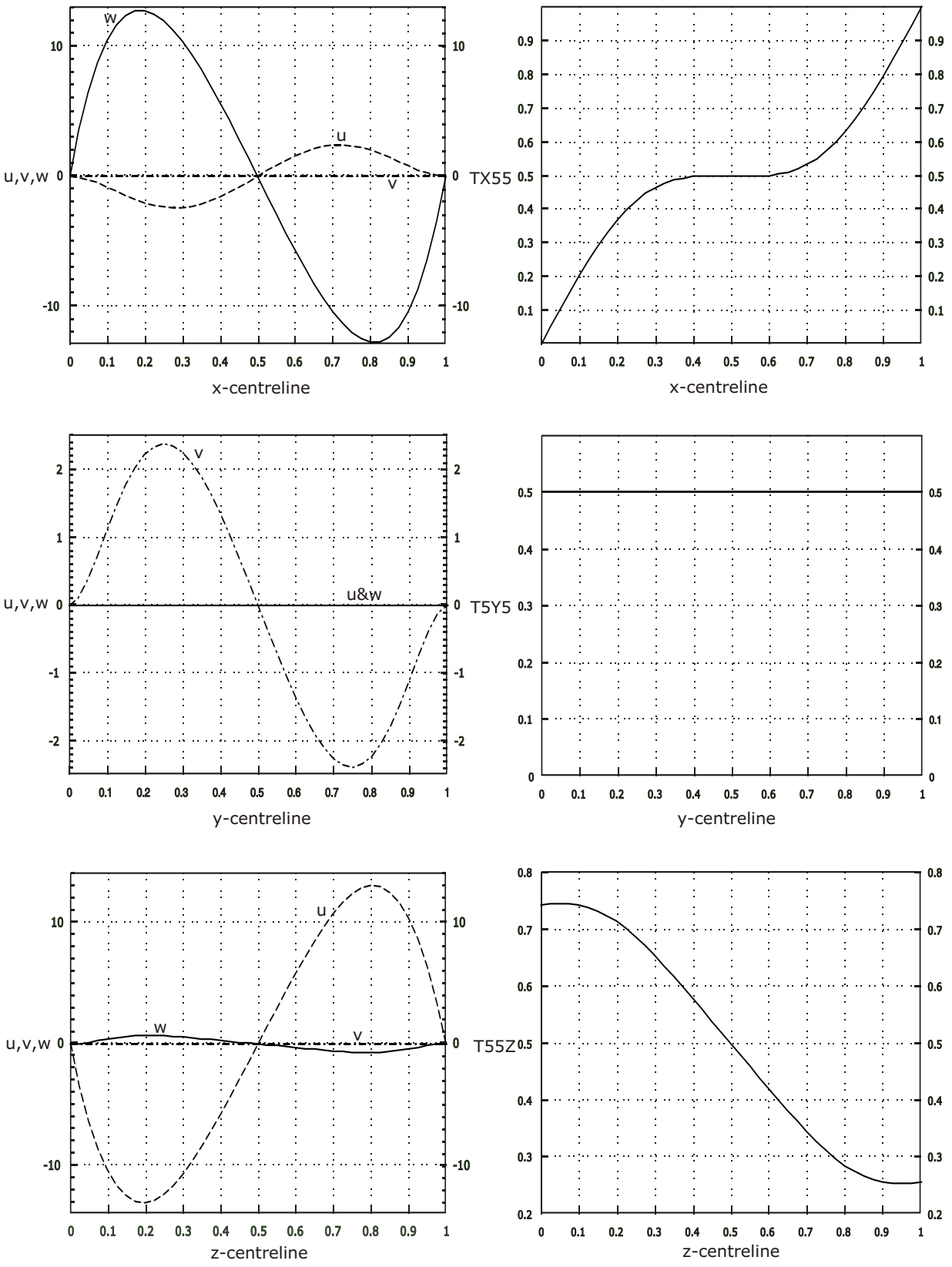

Figure 8. Velocity and temperature profiles on the centrelines of the cube for solution corresponding to family B. *Ra*=6000, *Pr*=1.0. Frames to the left indicate velocity profiles and frames to the right indicate temperature profiles.

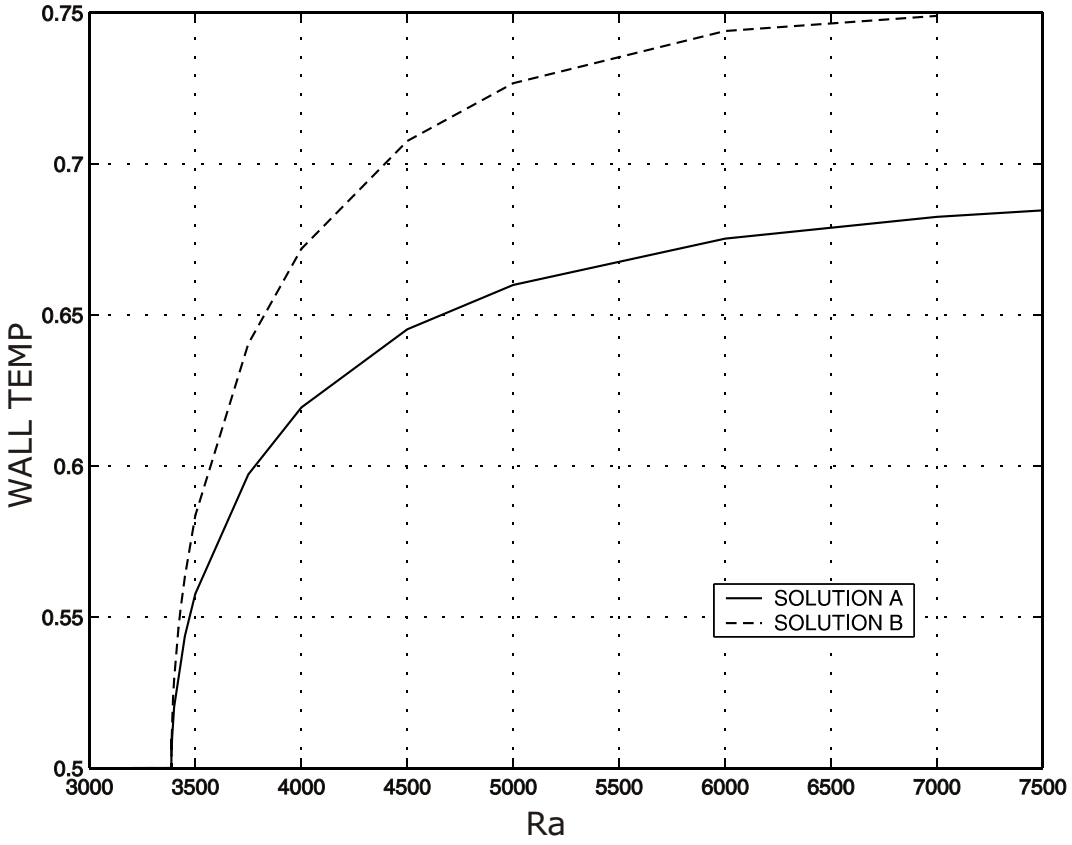

Figure 9. Bifurcation diagram Wall temperature at $z = 0$, $x = y = 0.5$, when Ra is increased. $Pr = 1$. At $(Ra)_{crit} = 3386.75$ pure conduction solution bifurcates into convective solutions.

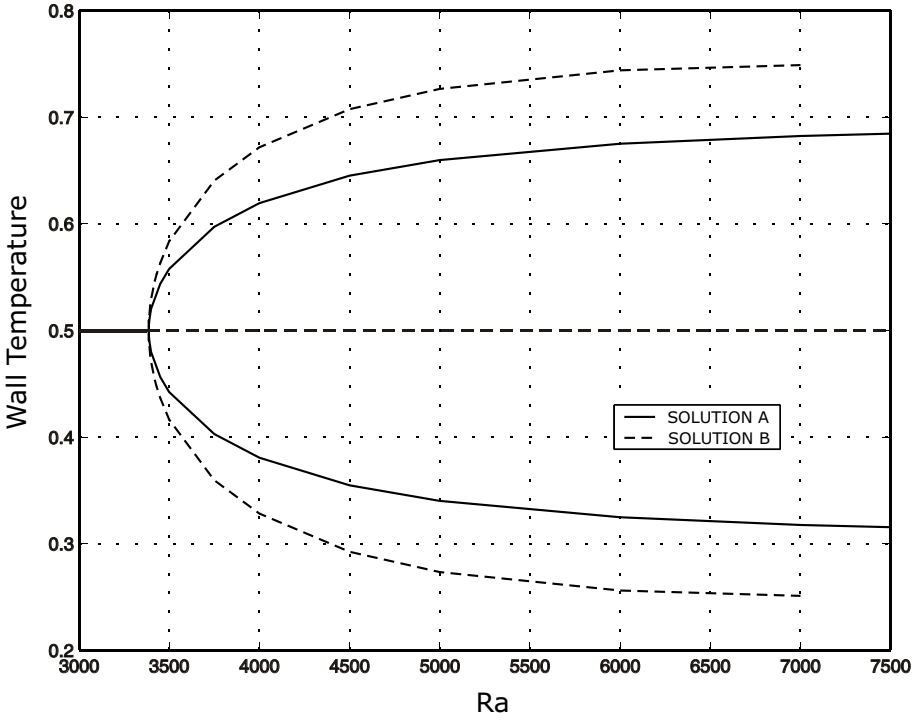

Figure 10. Bifurcation diagram including the solutions obtained due to symmetry also.(a) For wall temperature at $z = 0$, $x = y = 0.5$.

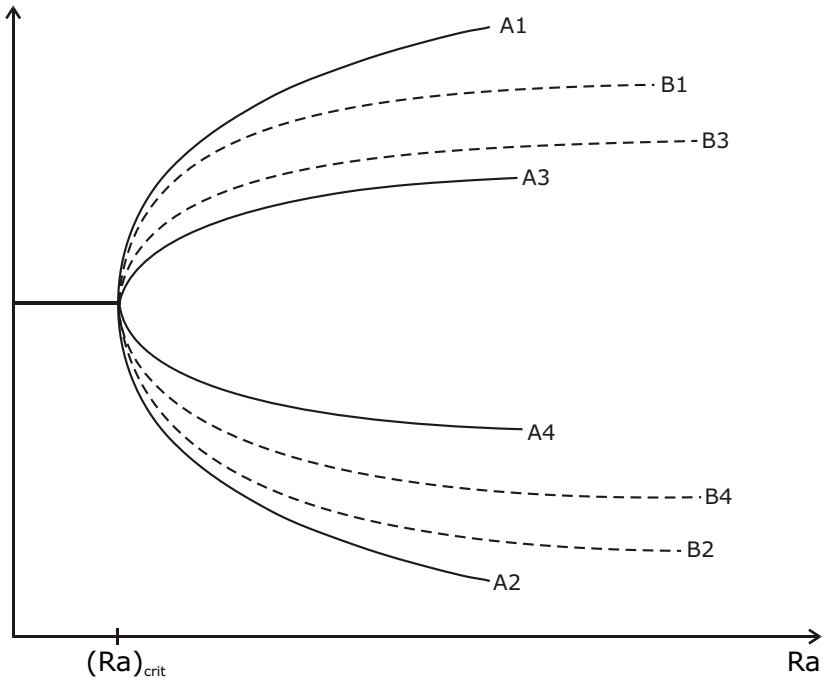

Figure 10(b) Schematic diagram for any quantity showing all eight solutions in the two families.

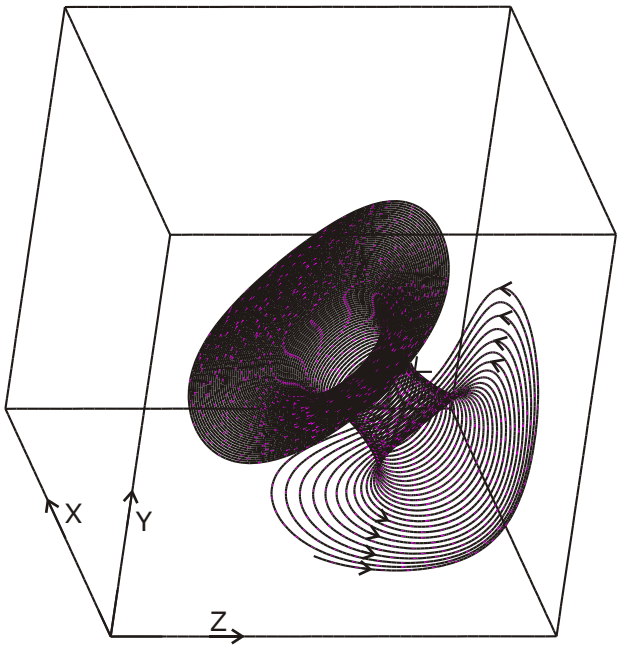

Figure 11. Streamlines for a case close to the critical Rayleigh number. *Ra*=3388, *Pr*=1.0. (a) Family A solution.

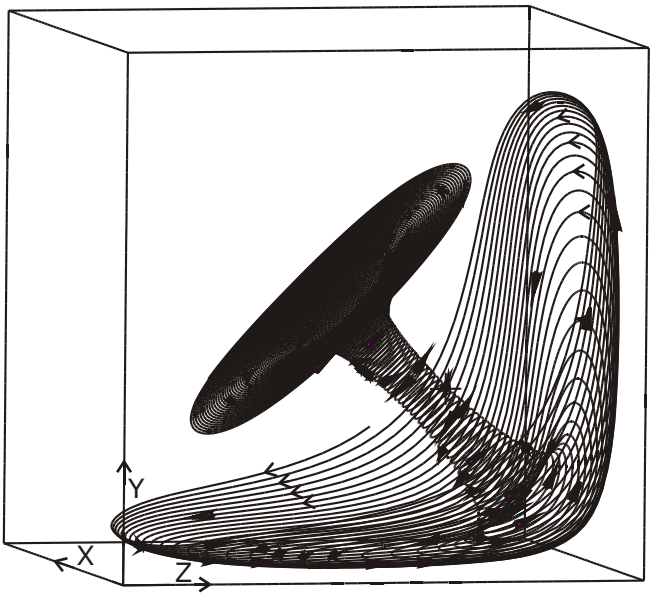

Figure 11(b) Family A solution.

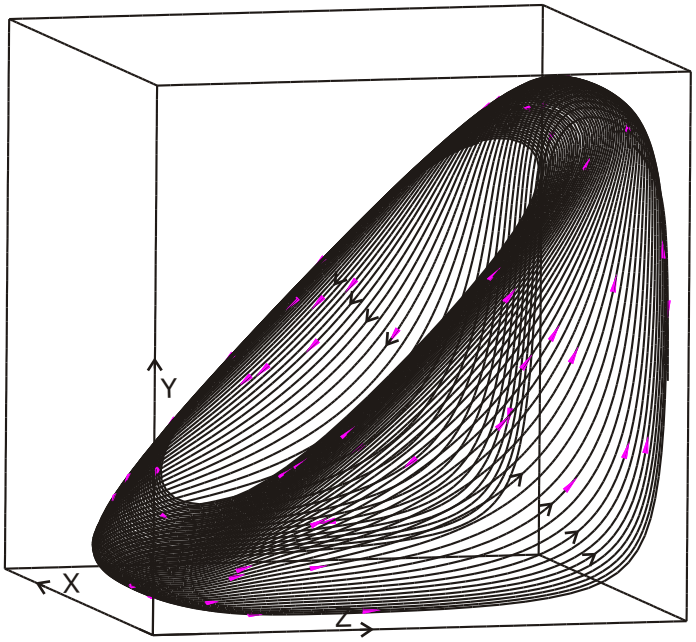

Figure 11(c) Family A solution.

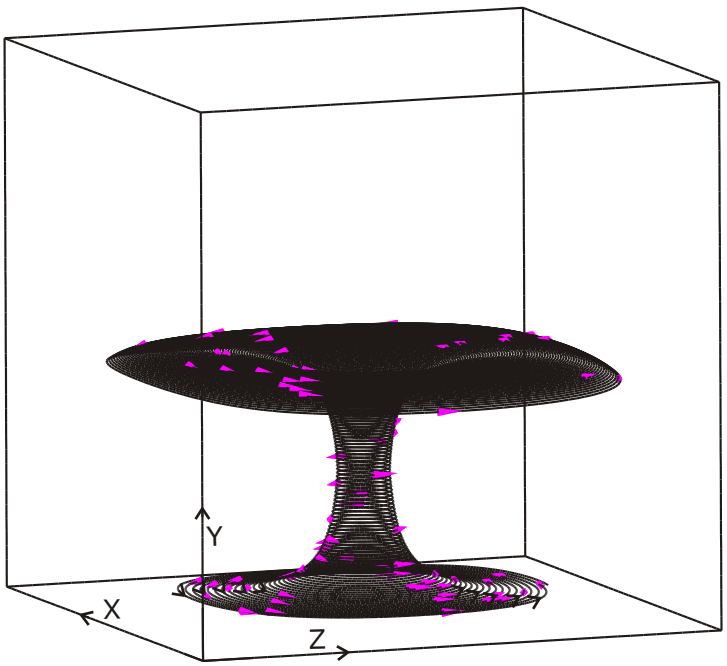

Figure 11(d) Family B solution.